Amelioration of muscular dystrophy by transgenic expression of Niemann-Pick C1

Michelle S. Steen, Marvin E. Adams, Yan Tesch, and Stanley C. Froehner*

Department of Physiology & Biophysics, University of Washington, Seattle WA 98195

Running Head: Niemann-Pick C1 and muscular dystrophy

*Corresponding Author
Department of Physiology & Biophysics, Box 7290
University of Washington
Seattle WA 98195-7290
(206) 543-0950
Froehner@u.washington.edu

Abbreviations:
DMD - Duchenne muscular dystrophy
DPC - dystrophin-associated protein complex
TA - tibialis anterior

Abstract

Duchenne muscular dystrophy (DMD) and other types of muscular dystrophies are caused by the loss or alteration of different members of the dystrophin protein complex. Understanding the molecular mechanisms by which dystrophin-associated protein abnormalities contribute to the onset of muscular dystrophy may identify new therapeutic approaches to these human disorders. By examining gene expression alterations in mouse skeletal muscle lacking α-dystrobrevin (*Dtna*$^{-/-}$), we identified a highly significant reduction of the cholesterol trafficking protein, Niemann-Pick C1 (NPC1). Mutations in NPC1 cause a progressive neurodegenerative, lysosomal storage disorder. Transgenic expression of NPC1 in skeletal muscle ameliorates muscular dystrophy in the *Dtna*$^{-/-}$ mouse (which has a relatively mild dystrophic phenotype) and in the *mdx* mouse, a model for DMD. These results identify a new compensatory gene for muscular dystrophy and reveal a potential new therapeutic target for DMD.

Duchenne muscular dystrophy (DMD) is a fatal, muscle wasting disease, affecting approximately 1 in 3500 live male births. Patients with DMD display muscle weakness early in life, experience progressive loss of mobility due to severe muscle degeneration and ultimately die in the early twenties, usually from respiratory or cardiac failure. DMD results from the loss of functional dystrophin, a large intracellular membrane protein required for the formation of the dystrophin-associated protein complex (DPC), a large complex of transmembrane glycoproteins (Ervasti *et al.*, 1990), adaptor proteins, and signaling proteins (Hoffman *et al.*, 1987). Despite significant advances in gene therapy aimed at replacing the defective dystrophin gene (Cox *et al.*, 1993; Ragot *et al.*, 1993; Wang *et al.*, 2000; Gregorevic *et al.*, 2006), DMD still remains without an effective treatment.

The DPC forms a physical link between the intracellular actin cytoskeleton and the extracellular matrix. Members of the DPC include the dystroglycans (which provide transmembrane linkage between dystrophin and laminin), γ-actin, the sarcoglycans, and the syntrophin-dystrobrevin scaffold for signaling proteins (Ervasti, 2007). Mutations in DPC proteins cause other forms of muscular dystrophies, such as the limb-girdle muscular dystrophies (Ozawa *et al.*, 2005). Although the DPC complex has been extensively studied, the downstream molecular and cellular alterations that lead to muscle degeneration in DMD are largely unknown. A more complete understanding of these pathways may reveal new therapeutic targets that slow the progression of muscle degeneration.

In this study, we performed gene expression analyses on skeletal muscle from mice lacking α-dystrobrevin (*Dtna*$^{-/-}$), which display a mild dystrophic phenotype compared to *mdx* mice (Grady *et al.*, 1999), in order to identify new genes contributing to muscular dystrophy. The *Dtna*$^{-/-}$ mice have a highly significant reduction in Niemann-Pick C1 (*Npc1*) transcript and protein. Mutations in *Npc1* are responsible for NPC1 disease, a progressive and ultimately fatal, autosomal recessive, neurodegenerative disease, affecting ~1 in 150,000 live births. The function of NPC1 is not well understood but appears to be involved in regulating intracellular cholesterol transport (Liscum *et al.*, 1989). Cells lacking NPC1 exhibit an accumulation of LDL-derived unesterified cholesterol in the endosomal/lysosomal pathway, which may impair trafficking or other cellular functions (Sokol *et al.*, 1988). NPC1 has been studied extensively in brain and liver, the tissues more severely affected by the disease. The role of NPC1 in skeletal muscle has not been examined, to our knowledge.

To determine if the restoration of NPC1 improves the health of dystrophic muscle, we expressed *Npc1* in skeletal muscle of both *Dtna*$^{-/-}$ and *mdx* mice. Here, we show that NPC1 expression in skeletal muscle significantly ameliorates the dystrophic phenotype in both of these mouse models of muscular dystrophy. These findings identify NPC1 as a booster gene for compromised muscle (Engvall and Wewer, 2003) and reveal a potential new therapeutic target for muscular dystrophies.

Materials and Methods

Animals. Mice lacking dystrophin (*mdx*) and mice heterozygous for the Niemann Pick type C1 mutant allele were obtained from the Jackson Laboratory (Bar Harbor, Maine). The NPC1 mutant allele contains the insertion of a retroposon, resulting in a premature truncation, deleting 11 out of the 13 transmembrane domains. Breeding pairs were bred to produce *Npc1*-null ($Npc1^{-/-}$), heterozygous ($Npc1^{+/-}$), and wild-type ($Npc1^{+/+}$) offspring. Genotyping was performed according to Jackson Laboratory protocols (jaxmice.jax.org). $Dtna^{-/-}$ mice were a generous gift of Joshua Sanes (Harvard University). All animal experiments were performed with the approval of the Institutional Animal Care and Use Committee at the University of Washington.

Affymetrix GeneChip Assays

Quadriceps muscles were dissected from six-week-old male $Dtna^{-/-}$ and their wild-type, sex-matched littermates. Total RNA was isolated from each quadriceps muscle using Trizol Reagent (Invitrogen) and the RNeasy Mini Kit (Qiagen). For each sample, 20 μg of total RNA was processed for gene expression analysis, using Affymetrix Murine Genome U74Av2, U74Bv2, and U74Cv2 arrays, following Affymetrix protocols (www.affymetrix.com). RNA from eight experimental and eight control mice was analyzed individually on the U74v2 arrays. Double-stranded cDNA was synthesized from total RNA (SuperScript Choice system, Invitrogen). Single-stranded, biotin-labeled cRNA (BioArray™ HighYield™ RNA Transcript Labeling Kit (T7), Enzo Life Sciences) was synthesized by *in vitro* transcription, and fragmented. The resulting fragmented, biotin-labeled cRNA (15 μg) was hybridized to the Affymetrix arrays, which were labeled

with the GeneChip® Fluidics Station 400 (Affymetrix) and scanned with the GeneChip® Scanner 3000 (Affymetrix) at the Center for Array Technologies at the University of Washington. Initial data analysis was performed with Affymetrix® Microarray Suite 5.0.

Real-Time quantitative RT-PCR. Real-Time quantitative RT-PCR was performed using TaqMan® chemistry and the ABI 7000 sequence detection system (Applied Biosystems). Quadriceps muscles were dissected from six-week-old male *Dtna*$^{-/-}$ mice and their wild-type, sex-matched littermates. Real-Time quantitative RT-PCR was performed on each sample using 50 ng of RNA, One-Step RT-PCR Master Mix reagents (Applied Biosystems), and *Npc1* primers (5'-AATGCGGTCTCCTTGGTCAA-3' and 5'-GCTCTCGTTATATGGCTGCAGAA-3', Integrated DNA Technologies) and probe (5' 6-FAM d(CACAGAAATGCCACAGCTCATCACCAA) BHQ-1 3', Biosearch Technologies, Inc.), or control 18S primers and probe (Applied Biosystems, P/N 4310893E). The relative expression of *Npc1* mRNA was normalized to 18S RNA in the same sample. Each sample was run in duplicate.

Generation of NPC1 antibody. A 16-amino acid peptide (KAKRHTTYERYRGTER), corresponding to the cytosolic carboxy-terminal domain of murine NPC1 (GenBank Acc. No. BC052437, residues 1256-1271) was synthesized (Macromolecular Resources, Colorado State University), conjugated to keyhole limpet hemocyanin (Pierce), and injected into New Zealand White rabbits (Covance Research Products). Antibodies were affinity purified using peptide bound to UltraLink Iodoacetyl Gel columns (Pierce).

Membrane enrichment and immunoblots. Tissues were dissected and quick frozen in liquid nitrogen. Membrane preparations and immunoblotting were performed as described previously(Garver *et al.*, 2000) with the following modifications. Tissues were

homogenized in buffer A (25 mM MES, pH 6.5, 150 mM NaCl, and protease inhibitors (Sigma, St. Louis)) and centrifuged for 30 min at 100,000 *g*, generating a cytosolic fraction (supernatant) and membrane-enriched fraction (pellet). Pellets were resuspended in buffer A plus 1% Triton X-100 and centrifuged at 2000 X *g* for 10 min. Protein content was determined using the bicinchoninic acid protein assay (Pierce). Gels (4-15% or 4-20% Tris-HCl gradient, BioRad) were loaded with 5-25 μg of protein and run and transferred to nitrocellulose membrane (Millipore). Primary antibody was detected using HRP-conjugated secondary antibody (Jackson ImmunoResearch Laboratories) and SuperSignal® West Femto Maximum Sensitivity Substrate (Pierce) using a CCD camera (AlphaInnotech).

Immunofluorescence microscopy. Single muscle fiber preparations were adapted from Percival et al. (2007). The fibers were incubated for 45 min in Alexa-Fluor-488-conjugated donkey anti-rabbit secondary antibody (Molecular Probes) diluted in blocking buffer (0.05% saponin, 10% goat serum in phosphate buffered saline) and washed. Labeled fibers were separated on glass slides in ProLong® Gold antifade mounting media, containing DAPI (Invitrogen) for visualization of nuclei. Confocal microscopy images were obtained using a Zeiss LSM 510 META at the W.M. Keck Center for Advanced Studies in Neural Signaling at the University of Washington. Stacks of 40 serial optical sections measuring 0.44 μm in thickness were obtained at 0.44 μm intervals through the muscle fibers, using a Plan-Neofluar 40x/1.3 Oil objective at 2x zoom. The sections were merged into a single image using the “maximum” projection method.

Filipin staining. Teased muscle fibers were incubated with block solution (0.2% bovine serum albumin, 0.2% fish skin gelatin (Sigma) in phosphate buffered saline) for 20 min. The fibers were stained with block solution containing 1 mg/ml filipin (Sigma) according to the method of Carozzi et al. (2000). Fibers were imaged using a Zeiss Axioskop 2 microscope.

Generation of transgenic mice. The cDNA encoding full-length *Npc1* was obtained from ATCC (cat. no. 9890203). Upon sequence comparison of this clone (GenBank BC052437) with that of mouse *Npc1* sequence (GenBank AF003348), multiple ESTs, and the mouse genome, we observed several sequence discrepancies. We considered the consensus sequence generated from all of the sequences to be correct. Therefore, by PCR, we made a single base mutation, a3963g, resulting in an amino acid alteration, K1273E, to match the ATCC sequence to that of the consensus. The *Npc1* cDNA was cloned into the NotI site of pBSX-HSAvpA (Crawford *et al.*, 2000)**,** a generous gift from Dr. Jeffrey Chamberlain, University of Washington. The linearized construct was injected into the pronuclei of *C57BL/6 x C3H* embryos (University of Washington, Department of Comparative Medicine, Transgenic Resources Program), and the resulting progeny were genotyped by PCR (5'-GATGAA GCAGACAGTATTCAGC-3' and 5'-CAGTTCGGCTCGCGGAGCAC-3'). Four founder lines carrying the *Npc1* transgene were identified (Tg(*Npc*1)) and bred onto *Dtna*$^{-/-}$ (*Dtna*$^{-/-}$-Tg(*Npc*1) and *mdx* (*mdx*-Tg(*Npc*1)) backgrounds.

Central nuclei counts and fiber diameter measurements. Tibialis anterior (TA), soleus, and diaphragm muscles were dissected, embedded in O.C.T. (TissueTek) and quick-frozen in liquid nitrogen-cooled isopentane. Cross-sections (8 μm) taken from the

mid-belly of the muscles were fixed in 95% ethanol and stained with Gill's No. 3 hematoxylin and eosin Y. Microscope (Zeiss Axioskop 2) images of the entire muscle were used to assess the presence of centrally-located nuclei. A minimum of five mice per genotype was analyzed. *Dtna*$^{-/-}$-Tg(*Npc*1) were examined at three months of age, and *mdx*-Tg(*Npc*1) at eight weeks of age. ImageJ software was used to measure Feret's diameter (Briguet *et al.*, 2004) of muscle fibers**.** Measurements were taken from an entire cross-section of soleus muscle from each of three mice per genotype examined. Coefficients of variation (%) of the fiber diameters were calculated as standard deviation of the muscle fiber size/ mean fiber size x 100.

Creatine kinase assay. Blood (50-100μl) was collected from the saphenous vein and allowed to clot for 20 min. Serum was obtained following centrifugation of the blood at 5,000g for 8 min at room temperature. We used the CK Liquid-UV Test (StanBio) and followed the manufacturer's protocol for the determination of serum creatine kinase activity. A minimum of five mice per genotype was analyzed.

Statistical analyses. For statistical analyses of microarray data, two-tailed Student's paired *t* tests were performed on the signal intensities of all probe sets to identify significant differences between the control and experimental groups. A value of $p<0.005$ was considered significant. A two-tailed Student's paired *t* test was performed on the quantitative RT-PCR data to determine the significance of the difference in *Npc1* expression between the control and experimental groups. We performed one-way ANOVA tests with Tukey's post test for determination of statistical significance of both central nucleation and creatine kinase activity, using GraphPad Prism version 4.00 (GraphPad Software, San Diego, California).

RESULTS

Gene expression array analysis of *Dtna*$^{-/-}$ muscle

To identify genes with altered expression in a mouse model of muscular dystrophy, we compared gene expression levels from muscle of *Dtna*$^{-/-}$ mice to littermate controls. The *Dtna*$^{-/-}$ mouse was chosen for these studies because its mild dystrophy does not evoke the aggressive immune response that predominates gene expression analysis studies in *mdx* muscle (Porter *et al.*, 2002). The goal of these studies was to identify genes with expression altered prior to the onset of muscle degeneration. To improve the probability of identifying early gene expression changes, we used relatively young mice (6 weeks) and selected a muscle (quadriceps) that is only mildly affected (based on histological analysis). We analyzed large numbers of muscle samples independently so that even small, but statistically significant changes would be revealed. Using this approach, we identified more than 200 transcripts that were differentially regulated in *Dtna*$^{-/-}$ muscle (**Supplementary Tables 1 & 2**). Because of its high level of statistical significance ($p = 3.0e^{-7}$) and its involvement in a known neurodegenerative disease, our attention was directed toward the gene encoding *Npc1*. The array data indicated that the expression level of *Npc1* transcript is reduced by approximately 50% in the *Dtna*$^{-/-}$ muscle (**Supplementary Table 1**). We used real-time quantitative RT-PCR to confirm the 50% reduction ($p<0.05$) of *Npc1* transcript in *Dtna*$^{-/-}$ quadriceps muscle (**Fig. 1**).

Since reduction in mRNA does not necessarily lead to a reduction in protein levels we compared NPC1 protein levels in wild type and *Dtna*$^{-/-}$ muscle (**Fig 1**). Like the *Npc1* transcript levels, NPC1 protein levels are also markedly decreased in *Dtna*$^{-/-}$ muscle,

compared to wild-type samples. This was particularly evident in the membrane-enriched samples as expected for the transmembrane NPC1 (**Fig. 1**).

We used immunofluorescence to determine the location of NPC1 in skeletal muscle (**Fig 2**). Labeling of individual muscle fibers using our NPC1 antibody showed a specific punctate pattern not present in the NPC1 knockout muscle. This labeling colocalized with Lamp, a lysosomal marker (**Fig. 2**).

Production of transgenic NPC1 mice

Having established that the levels of NPC1 were reduced in the *Dtna*$^{-/-}$ mouse model of muscular dystrophy, we hypothesized that restoration of skeletal muscle NPC1 levels could ameliorate the dystrophic phenotype. We tested this hypothesis by generating transgenic mice expressing *Npc1* in specifically in skeletal muscle. We obtained four lines of transgenic NPC1 mice (Tg(*Npc1*)19, Tg(*Npc1*)55, Tg(*Npc1*)56, and Tg(*Npc1*)58). Two of these transgenic lines (Tg(*Npc1*)19 and Tg(*Npc1*)58) showed high expression of NPC1 in skeletal muscle (**Fig. 3**). The transgenic mice showed no adverse effects of high levels on NPC1 in muscle. Expression of the NPC1 transgene results in a qualitative increase in the number of visible puncta but no increase in diffuse or sarcolemma labeling (**Supplementary Fig. 1**). Each of the four Tg(*Npc1*) lines was crossed onto the *Dtna*$^{-/-}$ and onto the *mdx* backgrounds.

Muscular dystrophy is characterized, in part, by increased numbers of regenerating muscle fibers (identified by central nucleation) and damaged muscle membranes. The latter leads to elevated levels of serum creatine kinase, which

provides a body-wide assessment of myofiber sarcolemmal integrity. We assessed the effect of NPC1 expression on muscular dystrophy using these two parameters.

Transgenic NPC1 on *Dtna*$^{-/-}$ Background

We determined the percentage of centrally-nucleated muscle fibers from H&E-stained cross-sections of a predominantly slow-twitch (soleus), fast-twitch (TA), and respiratory (diaphragm) muscles of each genotype (**Fig. 4**). In both the soleus and diaphragm muscles, transgenic expression of NPC1 restored central nuclei counts to wild-type levels. High expression of transgenic NPC significantly reduced the percentage of centrally-nucleated myofibers by 83% (*Dtna*$^{-/-}$-Tg(*NPC1*)19) and 76% (*Dtna*$^{-/-}$-Tg(*NPC1*)58) relative to *Dtna*$^{-/-}$. We also observed smaller, but still statistically significant, reductions (40% and 34%) in the two lines expressing NPC1 at lower levels (*Dtna*$^{-/-}$-Tg(*NPC1*)55 and *Dtna*$^{-/-}$-Tg(*NPC1*)56, respectively) (data not shown). In diaphragm, central nuclei counts were significantly reduced in the two high NPC1-expressing transgenic lines (*Dtna*$^{-/-}$-Tg(*NPC1*)19 (89%) and *Dtna*$^{-/-}$-Tg(*NPC1*)58 (93%)) but the two transgenic lines expressing NPC1 at low levels did not show significant decreases (data not shown). In the TA muscle, the percentage of myofibers with central nuclei was not significantly changed in all four transgenic lines compared to *Dtna*$^{-/-}$ mice (**Fig. 4**; data not shown).

Dtna$^{-/-}$ transgenic mice expressing high levels of NPC1 also exhibited marked reductions in serum creatine kinase activity. As shown in **Fig. 4**, transgenic expression of NPC1 in *Dtna*$^{-/-}$ mice restored creatine kinase levels to wild-type levels in both the *Dtna*$^{-/-}$-Tg(*NPC1*)19 and *Dtna*$^{-/-}$-Tg(*NPC1*)58 lines. The reduced number of central nuclei and reduced serum creatine kinase levels demonstrate that the dystrophic

phenotype in the *Dtna*$^{-/-}$ *mouse* is ameliorated by transgenic skeletal muscle expression of NPC1. This amelioration is dose dependent and the degree of amelioration varies among the muscle fiber type.

Transgenic NPC1 on *mdx* Background

To determine if high expression of NPC1 alters the phenotype in a model of severe muscular dystrophy, we used the *mdx* mouse, a mouse studied extensively as a model of DMD (Bulfield *et al.*, 1984). All four transgenic NPC1 lines were bred onto the *mdx* background (**Fig. 5**). The extent of muscular dystrophy was assessed in eight-week-old wild-type, *mdx*, and *mdx*-Tg(*Npc1*) mice by quantifying the percentage of centrally-nucleated myofibers, determining serum creatine kinase activity and by measuring myofiber size variability (**Figs. 5**).

In muscles of the soleus, TA, and diaphragm, high expression of NPC1 significantly reduced the percentage of centrally-nucleated fibers relative to muscles from *mdx* mice (**Fig. 5**). Transgenic expression of NPC1 in *mdx* mice also significantly reduced serum creatine kinase levels (**Fig. 5**). Both of the transgenic lines expressing NPC1 at high levels (*mdx*-Tg(*Npc1*)19 and *mdx*-Tg(*Npc1*)58) showed sharply decreased creatine kinase levels (by 54% and 75%, respectively) compared to *mdx*. In fact, creatine kinase levels in mdx-Tg(*Npc1*)58 mice were not significantly different than wild-type levels.

An additional characteristic of dystrophic muscle is marked variability in muscle fiber diameter. We determined the variability of fiber diameter in the soleus muscle of the *mdx*-Tg(*Npc1*)58 mouse since it appeared to be the most improved based on the degree of improvement in central nucleation and creatine kinase levels. Indeed, we

found that while fiber sizes varied significantly in the *mdx* soleus compared to wild-type, transgenic expression of NPC1 significantly reduced the size variability (**Figs. 5**). Taken together, these data demonstrate that high expression of NPC1 in *mdx* skeletal muscle can significantly improve the dystrophic phenotype in this mouse model of Duchenne muscular dystrophy.

DISCUSSION

We used gene expression profiling of *Dtna*$^{-/-}$ mouse muscle to identify downstream cellular and/or molecular alterations that result from the loss of α-dystrobrevin, and contribute to the onset of the muscular dystrophy of *Dtna*$^{-/-}$ mice. *Dtna*$^{-/-}$ muscle displays a milder dystrophic phenotype than *mdx* muscle (Grady *et al.*, 1999). Expression profiling studies of *mdx* muscle have yielded large changes associated with immune response and regeneration in the dystrophic muscle (Porter *et al.*, 2002; Porter *et al.*, 2004). To identify alterations in proteins and/or signaling pathways that lead to degeneration, we sought to minimize the influence of responses associated with inflammation and muscle repair by examining the less severely affected *Dtna*$^{-/-}$ quadriceps muscle at six weeks of age. We analyzed large numbers of samples independently so statistical significance of small changes could be assessed. Selection of important changes was based on statistical significance, rather than an arbitrary magnitude change.

We identified more than 200 differentially expressed transcripts in the *Dtna*$^{-/-}$ quadriceps muscle. Several of the genes with increased expression, such as IGF-II, are likely involved in muscle regeneration, similar to trends observed in publicly available

datasets (Gene Expression Omnibus database, http://www.ncbi.nlm.nih.gov/geo/) from expression analyses of other dystrophy models (Bakay *et al.*, 2002; Haslett *et al.*, 2002; Porter *et al.*, 2002; Tseng *et al.*, 2002). In this study however, we focused on Niemann Pick type C1 (*Npc1*), which showed a highly significant ($p=3.02e^{-7}$) ~50% decrease in transcript levels in *Dtna*$^{-/-}$ muscle. *Npc1* had previously not been associated with the muscular dystrophies. However, a search using Gene Expression Omnibus database revealed that *Npc1* transcript levels are decreased in muscles from *mdx* and dysferlin-null mice (Garver *et al.*, 2000; Tseng *et al.*, 2002; Wenzel *et al.*, 2005).

NPC1 is a multispan membrane protein, residing primarily in late endosomes/lysosomes (Higgins *et al.*, 1999; Neufeld *et al.*, 1999; Garver *et al.*, 2000) as well as the trans Golgi network (Higgins *et al.*, 1999) and caveolin-1 containing vesicles (Higgins *et al.*, 1999; Garver *et al.*, 2000). The absence of NPC1 results in intracellular accumulations of large amounts of unesterified cholesterol and glycosphingolipids in late endosomes/lysosomes. In skeletal muscle, we found that NPC1 is localized primarily in lysosomes. Although cholesterol has been shown to accumulate in every tissue of *Npc1*$^{-/-}$ mice, including skeletal muscle (Xie *et al.*, 1999), the accumulation could not be observed in skeletal muscle fibers stained with filipin (**Supplementary Fig. 2**). To our knowledge, neither the function of NPC1 in skeletal muscle, nor the effects of NPC1 deficiency in skeletal muscle have been examined.

In order to determine if the reduction of NPC1 contributes to the muscular dystrophy of the *Dtna*$^{-/-}$ mouse, we generated *Dtna*$^{-/-}$ mice expressing transgenic *Npc1* under the control of the human skeletal α-actin (HSA) promoter (Brennan and Hardeman, 1993). Many of the dystrophic characteristics normally seen in *Dtna*$^{-/-}$

muscle are ameliorated in *Dtna*$^{-/-}$-Tg(*Npc1*) mice. Serum creatine kinase levels and the percentage of centrally-nucleated fibers in *Dtna*$^{-/-}$ soleus and diaphragm muscles were restored to near normal levels by transgenic expression of NPC1. Perhaps more importantly, muscle-specific expression of NPC1 dramatically improved the phenotype of the more severely dystrophic *mdx* mice. Thus, our results suggest a new avenue for treatment of Duchenne muscular dystrophy in humans.

The loss or reduction of NPC1 by itself does not cause muscular dystrophy. We have examined several muscle types (TA, soleus, quadriceps, sternomastoid, and diaphragm) from 6-week-old *Npc1*$^{-/-}$, as well as 6- and 16-week-old *Npc*$^{+/-}$ mice, and have found no evidence of dystrophy in these mice (data not shown). However, we report here that transgenic expression of *Npc1* in *mdx* skeletal muscle ameliorates the dystrophic phenotype. Such an apparent paradox has also been observed in the case of nNOS. Neither nNOS-null mice (Chao *et al.*, 1998), nor α-syntrophin-null mice (Kameya *et al.*, 1999; Adams *et al.*, 2000), which have reduced nNOS levels, are dystrophic. Yet, *mdx* mice, which also have reduced levels of nNOS (Brenman *et al.*, 1995), are dystrophic, and transgenic expression of nNOS ameliorates the dystrophy in *mdx* mice (Wehling *et al.*, 2001). A “two-hit” hypothesis has been suggested as a possible explanation for the discrepancy between the effect of nNOS reduction in the nNOS-null mouse and *mdx* mouse (Rando, 2001). According to this hypothesis, defects of the DPC are likely to have more than one biochemical consequence. Individually, either consequence may result in cell damage but alone is not enough to cause cell death; however, together they result in the severe necrosis observed in dystrophic muscle. In the case of nNOS, the reduction of nNOS causes ischemia in

muscle as a result of the loss of protection to contraction-induced vasoconstriction ("first hit"), but DPC defects increase the vulnerability ("second hit") of the muscle to ischemia, causing injury to the muscle. While the loss of NPC1 alone may not be sufficient to cause muscle fiber degeneration, it may in the presence of DPC defects contribute to the pathophysiology of dystrophic muscle.

The mechanism by which NPC1 dysfunction causes neuronal degeneration in Niemann-Pick disease is not fully understood. However, molecular abnormalities in NPC1-null cells suggest possible links to known causes of muscle degeneration. One particularly intriguing connection involves the caveolins. Caveolin-3, the muscle-specific form, binds directly to the dystrophin complex members, β-dystroglycan (Sotgia *et al.*, 2000) and nNOS (Garcia-Cardena *et al.*, 1997; Venema *et al.*, 1997) at the sarcolemma (Song *et al.*, 1996), and is required for the correct targeting of the dystrophin complex to cholesterol-sphingolipid rafts/caveolae (Galbiati *et al.*, 2000).

A link between caveolin-3 regulation and the muscular dystrophies is well established. Muscles from Duchenne muscular dystrophy patients and mdx mouse muscles have elevated caveolin-3 levels (Repetto *et al.*, 1999; Vaghy *et al.*, 1998). Furthermore, mutations in caveolin-3 are the genetic basis for limb-girdle muscular dystrophy 1C (LGMD 1C) (Minetti *et al.*, 1998). Finally, a Duchenne-like muscular dystrophy results from transgenic overexpression of caveolin-3 in mouse muscle (Galbiati *et al.*, 2000).

Interestingly, elevated caveolin levels are also associated with NPC1 deficiency (Garver *et al.*, 1999; Garver *et al.*, 2002). In *Npc1*-heterozygous fibroblasts, caveolin levels are increased in plasma membrane caveolae (Garver *et al.*, 2002). Whether the

link between caveolin and NPC1 has a role in ameliorating the dystrophic phenotype in skeletal muscle requires further study.

We have identified a significant reduction of NPC1, a cholesterol and sphingolipid trafficking protein, in α-dystrobrevin-null skeletal muscle. Furthermore, we show that transgenic expression of *Npc1* in skeletal muscle ameliorates the dystrophic phenotype of both *Dtna*$^{-/-}$ and *mdx* mice, two models of muscular dystrophy. Because cholesterol is known to affect plasma membrane rigidity and lipid-protein interactions, and because caveolae are involved in intracellular signaling, alterations in the cholesterol content of sarcolemmae or caveolae could adversely affect the structural integrity of the sarcolemmae, the ability of the membranes to repair themselves (Hernandez-Deviez et al., 2007), and/or the localization/function of caveolar signaling proteins. The involvement of NPC1 offers new therapeutic targets for muscular dystrophies resulting from abnormalities of the dystrophin complex.

ACKNOWLEDGMENTS

We thank Josh Sanes and Mark Grady for providing the *Dtna*$^{-/-}$ mice and Jeff Chamberlain for the HSA expression vector. This research was supported by NIH grants P01 NS046788 and RO1 NS33145 to SCF.

References

Adams, M.E., Kramarcy, N., Krall, S.P., Rossi, S.G., Rotundo, R.L., Sealock, R., and Froehner, S.C. (2000). Absence of alpha-syntrophin leads to structurally aberrant neuromuscular synapses deficient in utrophin. J Cell Biol *150*, 1385-1398.

Bakay, M., Zhao, P., Chen, J., and Hoffman, E.P. (2002). A web-accessible complete transcriptome of normal human and DMD muscle. Neuromuscul Disord *12 Suppl 1*, S125-141.

Brenman, J.E., Chao, D.S., Xia, H., Aldape, K., and Bredt, D.S. (1995). Nitric oxide synthase complexed with dystrophin and absent from skeletal muscle sarcolemma in Duchenne muscular dystrophy. Cell *82*, 743-752.

Brennan, K.J., and Hardeman, E.C. (1993). Quantitative analysis of the human alpha-skeletal actin gene in transgenic mice. J Biol Chem *268*, 719-725.

Briguet, A., Courdier-Fruh, I., Foster, M., Meier, T., and Magyar, J.P. (2004). Histological parameters for the quantitative assessment of muscular dystrophy in the mdx-mouse. Neuromuscul Disord *14*, 675-682.

Bulfield, G., Siller, W.G., Wight, P.A., and Moore, K.J. (1984). X chromosome-linked muscular dystrophy (mdx) in the mouse. Proc Natl Acad Sci U S A *81*, 1189-1192.

Carozzi, A.J., Ikonen, E., Lindsay, M.R., and Parton, R.G. (2000) Role of Cholesterol in Developing T-Tubules:Analogous Mechanisms for T-Tubule and Caveolae Biogenesis. Traffic 1,326-341.

Chao, D.S., Silvagno, F., and Bredt, D.S. (1998). Muscular dystrophy in mdx mice despite lack of neuronal nitric oxide synthase. J Neurochem *71*, 784-789.

Cox, G.A., Cole, N.M., Matsumura, K., Phelps, S.F., Hauschka, S.D., Campbell, K.P., Faulkner, J.A., and Chamberlain, J.S. (1993). Overexpression of dystrophin in transgenic mdx mice eliminates dystrophic symptoms without toxicity. Nature *364*, 725-729.

Crawford, G.E., Faulkner, J.A., Crosbie, R.H., Campbell, K.P., Froehner, S.C., and Chamberlain, J.S. (2000). Assembly of the dystrophin-associated protein complex does not require the dystrophin COOH-terminal domain. J Cell Biol *150*, 1399-1410.

Engvall, E. and Wewer, U.M. (2003) The new frontier in muscular dystrophy research: booster genes. FASEB J. 17, 1579-2584.

Ervasti, J.M. (2007). Dystrophin, its interactions with other proteins, and implications for muscular dystrophy. Biochim Biophys Acta *1772*, 108-117.

Ervasti, J.M., Ohlendieck, K., Kahl, S.D., Gaver, M.G., and Campbell, K.P. (1990). Deficiency of a glycoprotein component of the dystrophin complex in dystrophic muscle. Nature *345*, 315-319.

Galbiati, F., Volonte, D., Chu, J.B., Li, M., Fine, S.W., Fu, M., Bermudez, J., Pedemonte, M., Weidenheim, K.M., Pestell, R.G., Minetti, C., and Lisanti, M.P. (2000). Transgenic overexpression of caveolin-3 in skeletal muscle fibers induces a Duchenne-like muscular dystrophy phenotype. Proc Natl Acad Sci U S A *97*, 9689-9694.

Garcia-Cardena, G., Martasek, P., Masters, B.S., Skidd, P.M., Couet, J., Li, S., Lisanti, M.P., and Sessa, W.C. (1997). Dissecting the interaction between nitric oxide

synthase (NOS) and caveolin. Functional significance of the nos caveolin binding domain in vivo. J Biol Chem *272*, 25437-25440.
Garver, W.S., Heidenreich, R.A., Erickson, R.P., Thomas, M.A., and Wilson, J.M. (2000). Localization of the murine Niemann-Pick C1 protein to two distinct intracellular compartments. J Lipid Res *41*, 673-687.
Garver, W.S., Hossain, G.S., Winscott, M.M., and Heidenreich, R.A. (1999). The Npc1 mutation causes an altered expression of caveolin-1, annexin II and protein kinases and phosphorylation of caveolin-1 and annexin II in murine livers. Biochim Biophys Acta *1453*, 193-206.
Garver, W.S., Krishnan, K., Gallagos, J.R., Michikawa, M., Francis, G.A., and Heidenreich, R.A. (2002). Niemann-Pick C1 protein regulates cholesterol transport to the trans-Golgi network and plasma membrane caveolae. J Lipid Res *43*, 579-589.
Grady, R.M., Grange, R.W., Lau, K.S., Maimone, M.M., Nichol, M.C., Stull, J.T., and Sanes, J.R. (1999). Role for alpha-dystrobrevin in the pathogenesis of dystrophin-dependent muscular dystrophies. Nature Cell Biol. *1*, 215-220.
Gregorevic, P., Allen, J.M., Minami, E., Blankinship, M.J., Haraguchi, M., Meuse, L., Finn, E., Adams, M.E., Froehner, S.C., Murry, C.E., and Chamberlain, J.S. (2006). rAAV6-microdystrophin preserves muscle function and extends lifespan in severely dystrophic mice. Nat Med *12*, 787-789.
Haslett, J.N., Sanoudou, D., Kho, A.T., Bennett, R.R., Greenberg, S.A., Kohane, I.S., Beggs, A.H., and Kunkel, L.M. (2002). Gene expression comparison of biopsies from Duchenne muscular dystrophy (DMD) and normal skeletal muscle. Proc Natl Acad Sci U S A *99*, 15000-15005.
Hernandez-Deviez, D.J., Howes, M.T., Laval, S.H., Bushby, K., Hancock, J.F., and Parton, R.G. (2007). Caveolin regulates endocytosis of the muscle repair protein, dysferlin. J Biol Chem.
Higgins, M.E., Davies, J.P., Chen, F.W., and Ioannou, Y.A. (1999). Niemann-Pick C1 is a late endosome-resident protein that transiently associates with lysosomes and the trans-Golgi network. Mol Genet Metab *68*, 1-13.
Hoffman, E.P., Brown, R.H., and Kunkel, L.M. (1987). Dystrophin: The protein product of the Duchenne muscular dystrophy locus. Cell *51*, 919-928.
Kameya, S., Miyagoe, Y., Nonaka, I., Ikemoto, T., Endo, M., Hanaoka, K., Nabeshima, Y., and Takeda, S. (1999). Alpha-syntrophin gene disruption results in the absence of neuronal-type nitric oxide synthase at the sarcolemma but does not induce muscle degeneration. J. Biol. Chem. *274*, 2193-2200.
Liscum, L., Ruggiero, R.M., and Faust, J.R. (1989). The intracellular transport of low density lipoprotein-derived cholesterol is defective in Niemann-Pick type C fibroblasts. J Cell Biol *108*, 1625-1636.
Minetti, C., Sotgia, F., Bruno, C., Scartezzini, P., Broda, P., Bado, M., Masetti, E., Mazzocco, M., Egeo, A., Donati, M.A., Volonte, D., Galbiati, F., Cordone, G., Bricarelli, F.D., Lisanti, M.P., and Zara, F. (1998). Mutations in the caveolin-3 gene cause autosomal dominant limb-girdle muscular dystrophy. Nat Genet *18*, 365-368.
Neufeld, E.B., Wastney, M., Patel, S., Suresh, S., Cooney, A.M., Dwyer, N.K., Roff, C.F., Ohno, K., Morris, J.A., Carstea, E.D., Incardona, J.P., Strauss, J.F., 3rd, Vanier, M.T., Patterson, M.C., Brady, R.O., Pentchev, P.G., and Blanchette-Mackie, E.J.

(1999). The Niemann-Pick C1 protein resides in a vesicular compartment linked to retrograde transport of multiple lysosomal cargo. J Biol Chem *274*, 9627-9635.
Ozawa, E., Mizuno, Y., Hagiwara, Y., Sasaoka, T., and Yoshida, M. (2005). Molecular and cell biology of the sarcoglycan complex. Muscle Nerve *32*, 563-576.
Percival, J.M., Gregorevic, P., Odom, G.L., Banks, G.B., Chamberlain, J.S., and Froehner, S.C. (2007). rAAV6-microdystrophin rescues aberrant Golgi complex organization in mdx skeletal muscles. Traffic *8*, 1424-1439.
Porter, J.D., Khanna, S., Kaminski, H.J., Rao, J.S., Merriam, A.P., Richmonds, C.R., Leahy, P., Li, J., Guo, W., and Andrade, F.H. (2002). A chronic inflammatory response dominates the skeletal muscle molecular signature in dystrophin-deficient mdx mice. Hum Mol Genet *11*, 263-272.
Porter, J.D., Merriam, A.P., Leahy, P., Gong, B., Feuerman, J., Cheng, G., and Khanna, S. (2004). Temporal gene expression profiling of dystrophin-deficient (mdx) mouse diaphragm identifies conserved and muscle group-specific mechanisms in the pathogenesis of muscular dystrophy. Hum Mol Genet *13*, 257-269.
Ragot, T., Vincent, N., Chafey, P., Vigne, E., Gilgenkrantz, H., Couton, D., Cartaud, J., Briand, P., Kaplan, J.C., Perricaudet, M., and et al. (1993). Efficient adenovirus-mediated transfer of a human minidystrophin gene to skeletal muscle of mdx mice. Nature *361*, 647-650.
Rando, T.A. (2001). Role of nitric oxide in the pathogenesis of muscular dystrophies: a "two hit" hypothesis of the cause of muscle necrosis. Microsc Res Tech *55*, 223-235.
Repetto, S., Bado, M., Broda, P., Lucania, G., Masetti, E., Sotgia, F., Carbone, I., Pavan, A., Bonilla, E., Cordone, G., Lisanti, M.P., and Minetti, C. (1999). Increased number of caveolae and caveolin-3 overexpression in Duchenne muscular dystrophy. Biochem Biophys Res Commun *261*, 547-550.
Sokol, J., Blanchette-Mackie, J., Kruth, H.S., Dwyer, N.K., Amende, L.M., Butler, J.D., Robinson, E., Patel, S., Brady, R.O., Comly, M.E., and et al. (1988). Type C Niemann-Pick disease. Lysosomal accumulation and defective intracellular mobilization of low density lipoprotein cholesterol. J Biol Chem *263*, 3411-3417.
Song, K.S., Scherer, P.E., Tang, Z., Okamoto, T., Li, S., Chafel, M., Chu, C., Kohtz, D.S., and Lisanti, M.P. (1996). Expression of caveolin-3 in skeletal, cardiac, and smooth muscle cells. Caveolin-3 is a component of the sarcolemma and co-fractionates with dystrophin and dystrophin-associated glycoproteins. J Biol Chem *271*, 15160-15165.
Sotgia, F., Lee, J.K., Das, K., Bedford, M., Petrucci, T.C., Macioce, P., Sargiacomo, M., Bricarelli, F.D., Minetti, C., Sudol, M., and Lisanti, M.P. (2000). Caveolin-3 directly interacts with the C-terminal tail of beta -dystroglycan. Identification of a central WW-like domain within caveolin family members. J Biol Chem *275*, 38048-38058.
Tseng, B.S., Zhao, P., Pattison, J.S., Gordon, S.E., Granchelli, J.A., Madsen, R.W., Folk, L.C., Hoffman, E.P., and Booth, F.W. (2002). Regenerated mdx mouse skeletal muscle shows differential mRNA expression. J Appl Physiol *93*, 537-545.
Vaghy, P.L., Fang, J., Wu, W., and Vaghy, L.P. (1998). Increased caveolin-3 levels in mdx mouse muscles. FEBS Lett *431*, 125-127.
Venema, V.J., Ju, H., Zou, R., and Venema, R.C. (1997). Interaction of neuronal nitric-oxide synthase with caveolin-3 in skeletal muscle. Identification of a novel caveolin scaffolding/inhibitory domain. J Biol Chem *272*, 28187-28190.

Wang, B., Li, J., and Xiao, X. (2000). Adeno-associated virus vector carrying human minidystrophin genes effectively ameliorates muscular dystrophy in mdx mouse model. Proc Natl Acad Sci U S A *97*, 13714-13719.
Wehling, M., Spencer, M.J., and Tidball, J.G. (2001). A nitric oxide synthase transgene ameliorates muscular dystrophy in mdx mice. J Cell Biol *155*, 123-131.
Wenzel, K., Zabojszcza, J., Carl, M., Taubert, S., Lass, A., Harris, C.L., Ho, M., Schulz, H., Hummel, O., Hubner, N., Osterziel, K.J., and Spuler, S. (2005). Increased susceptibility to complement attack due to down-regulation of decay-accelerating factor/CD55 in dysferlin-deficient muscular dystrophy. J Immunol *175*, 6219-6225.
Xie, C., Turley, S.D., Pentchev, P.G., and Dietschy, J.M. (1999). Cholesterol balance and metabolism in mice with loss of function of Niemann-Pick C protein. Am J Physiol *276*, E336-344.

Figure Legends

Figure 1. Reduction of *Npc1* mRNA and NPC1 protein in *Dtna*$^{-/-}$ quadriceps muscle. (**A**) Real-time RT-PCR was used to determine *Npc1* transcript levels (arbitrary units) in wild-type and . *Dtna*$^{-/-}$ quadriceps muscle. Data are shown as mean ± s.d. *p<0.05, vs. wild-type. (**B**) Immunoblot analysis of NPC1 levels in membrane-enriched fractions prepared from wild-type and *Dtna*$^{-/-}$ mouse quadriceps muscles. Two examples are shown.

Figure 2. NPC1 localizes to lysosomes in skeletal muscle. (**A**) Immunofluorescence of individual muscle fibers from wild-type and *Npc1*$^{-/-}$ quadriceps muscles. (**B**) Co-labeling of the lysosome marker LAMP1 (red) with NPC1 (green) in wild type muscle fibers. DAPI staining was used as a nuclei marker. Scale bar, 10μm.

Figure 3. Relative expression levels of *Npc1* in transgenic lines.
Immunoblot analysis of NPC1 expression in diaphragm muscle homogenates from wild-type and four lines of *Dtna*$^{-/-}$-Tg(*Npc1*) mice. For comparison, 20 μg of wild-type whole muscle homogenate was loaded versus 5 μg for the *Dtna*$^{-/-}$-Tg(*Npc1*) mice. We estimate that transgenic expression levels of NPC1 are 2-4 fold (Tg55), 4-6 fold (Tg56) and 10-12 fold (Tg19 and Tg58) higher than wild type levels. GAPDH expression was determined on the same blot as a loading control (lower panel).

Figure 4. Amelioration of dystrophic phenotype in *Dtna*$^{-/-}$ muscle by transgenic expression of *Npc1*. (**A**) H&E staining of soleus cross-sections from wild-type, *Dtna*$^{-/-}$, and *Dtna*$^{-/-}$-Tg(*Npc1*)58 mice. Scale bar, 40 μm. (**B**) Percentage of myofibers with central nuclei (n ≥ 5 mice per genotype analyzed). (**C**) Serum creatine kinase levels. Data shown are mean ± s.d.. # $p<0.05$ vs. wild-type; * $p<0.05$ vs. *Dtna*$^{-/-}$. Data were collected from mice 3 months of age.

Figure 5. Transgenic expression of *Npc1* improves dystrophic phenotype of *mdx* mice. (**A**) H&E-stained cross-sections of soleus muscles from wild-type, *mdx*, and *mdx*-Tg(*Npc1*)58 mice. Scale bar, 40 μm. (**B**) Percentage of myofibers with central nuclei (n ≥ 5 mice per genotype). (**C**) Serum creatine kinase levels. (**D**,**E**) Quantitative analyses of fiber diameter in soleus muscles of wild-type, *mdx*, and *mdx*-Tg(*Npc1*)58 mice, determined using 'Feret's diameter' method. (**D**) Boxes represent the 25th to 75th percentiles and lines represent high and low values. Data were pooled from approximately 500 fibers from each of 3 mice per genotype. (**E**) Coefficients of variation of soleus fiber diameters. Each data point represents the variance coefficient calculated from each mouse. Lines represent means (dark bar) ± s.d. (error bars). (**A**,**C**) Data shown are mean ± s.d.. (**B,C**,**E**) # $p<0.05$ vs. wild-type; * $p<0.05$ vs. *mdx*. Data obtained from 8-week-old mice.

Figure S1. Expression of the transgene in mdx muscle fibers. Teased fibers from gastrocnemius muscle of mdx mice with and without transgenic NPC1 were labeled using the NPC1 antibody. Muscle fibers of mdx mice have a distribution of NPC1 similar to that seen in wild type muscle fibers (see Figure 2). Expression of the NPC1 transgene results in a qualitative increase in the number of visible puncta but no increase in diffuse or sarcolemma labeling. Scale bar, 10 μm.

Figure S2. Cholesterol distribution in muscle. Teased fibers from gastrocnemius muscle of the indicated mouse strain were stained with filipin. Although aggregations of cholesterol are observed in nerve/blood vessels, no significant accumulation of cholesterol was observed in the muscle fibers. Scale bar, 100 μm.

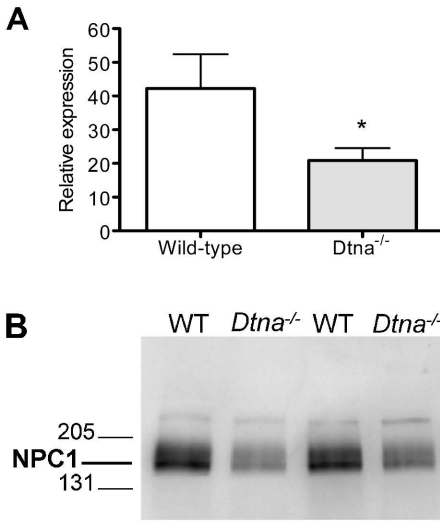
A
60
50
40
30
20
10
0
Relative expression
*
Wild-type
Dtna-/-
B
WT
Dtna-/-
WT
Dtna-/-
205
NPC1
131

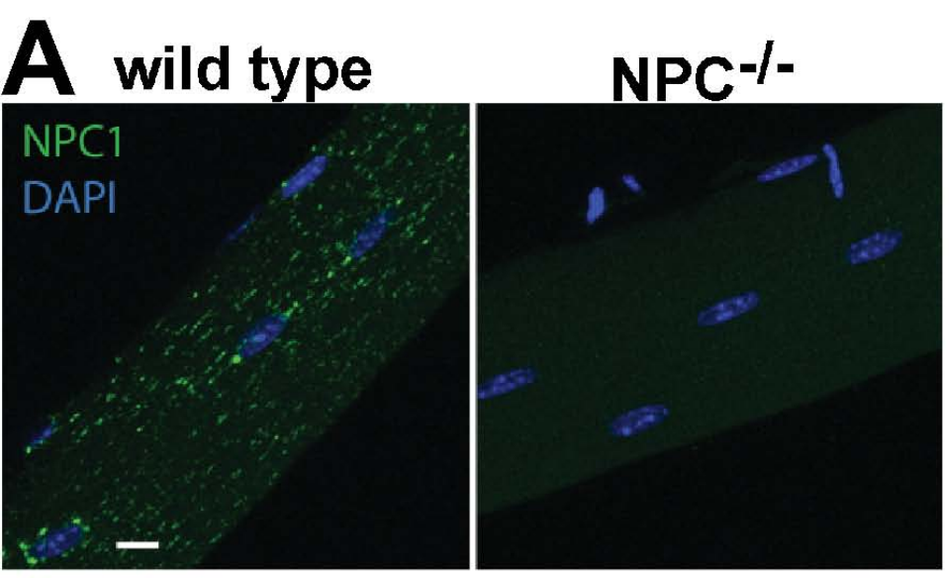
A
wild type
NPC-/-
NPC1
DAPI

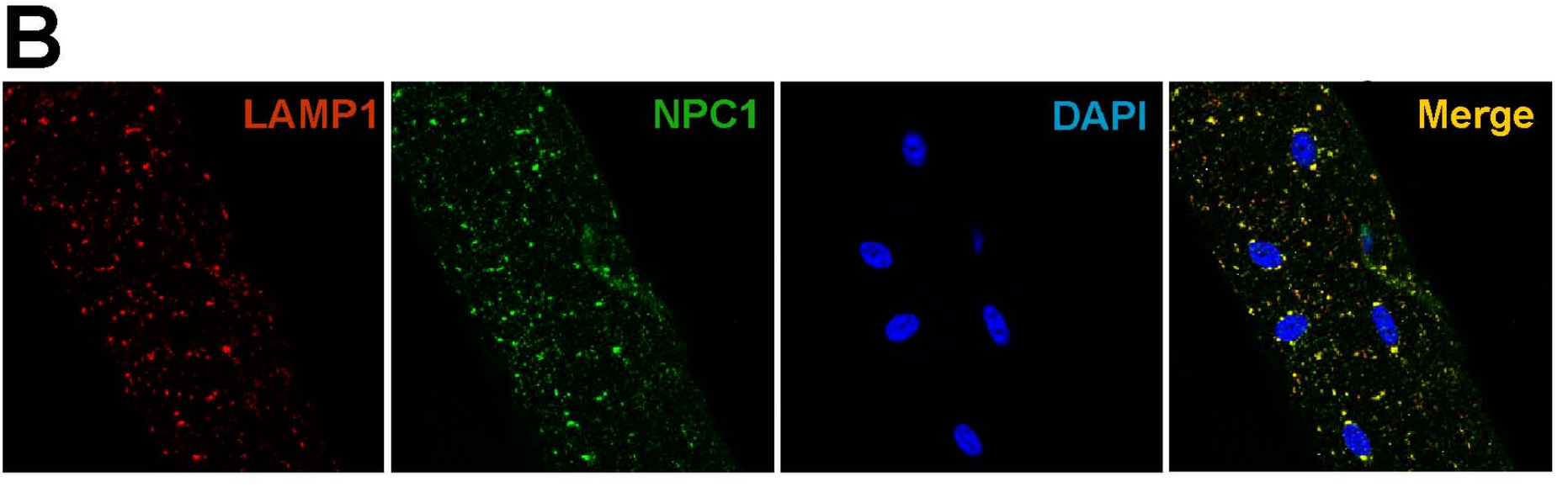
B
LAMP1
NPC1
DAPI
Merge

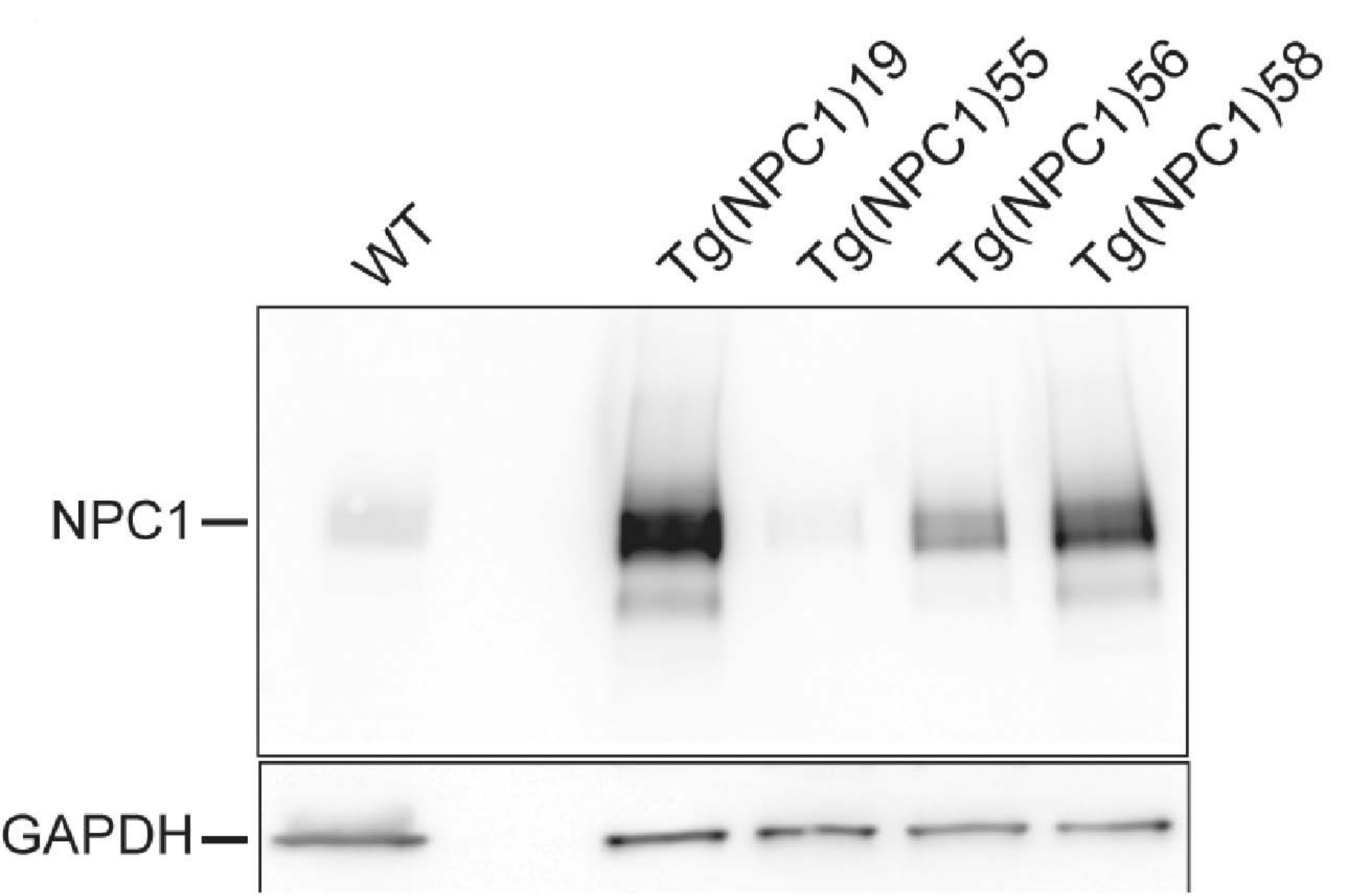
WT
Tg(NPC1)19
Tg(NPC1)55
Tg(NPC1)56
Tg(NPC1)58
NPC1
GAPDH

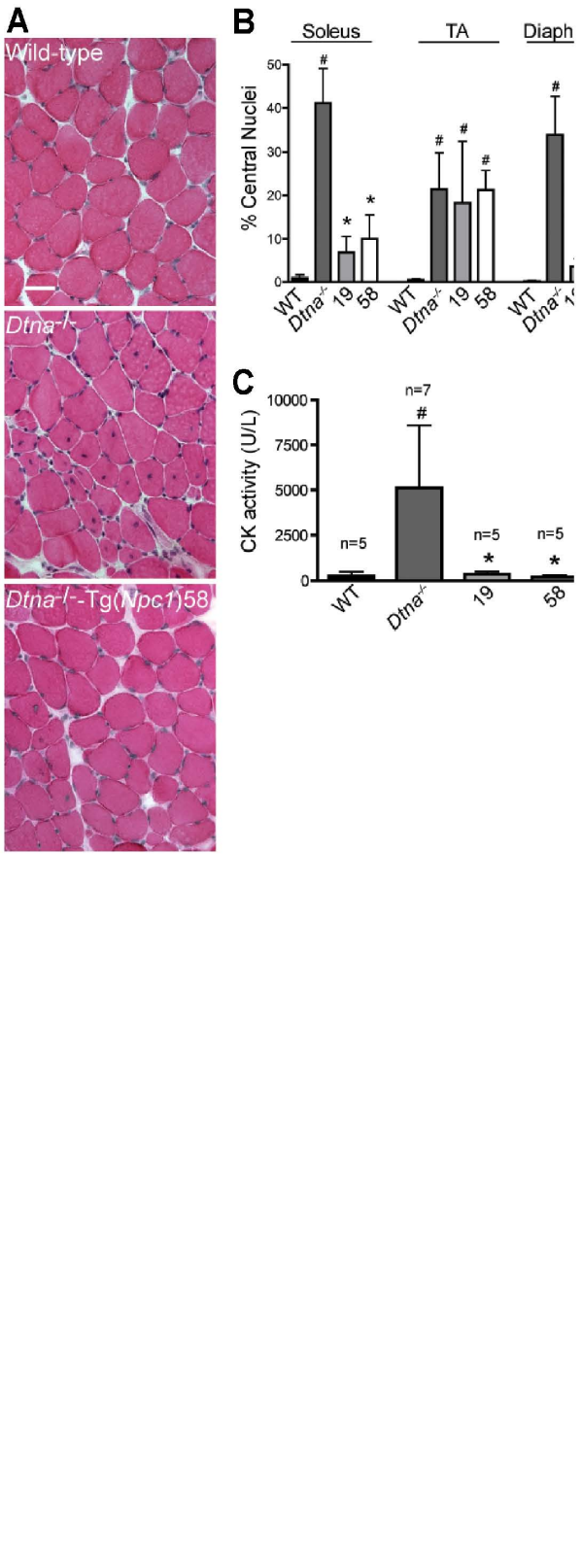
A
Wild-type
Dtna-/-
Dtna-/--Tg(Npc1)58
B
Soleus
TA
Diaph
% Central Nuclei
50
40
30
20
10
0
#
*
WT
Dtna-/-
19
58
C
CK activity (U/L)
10000
7500
5000
2500
0
n=7
n=5
n=5
n=5
WT
Dtna-/-
19
58

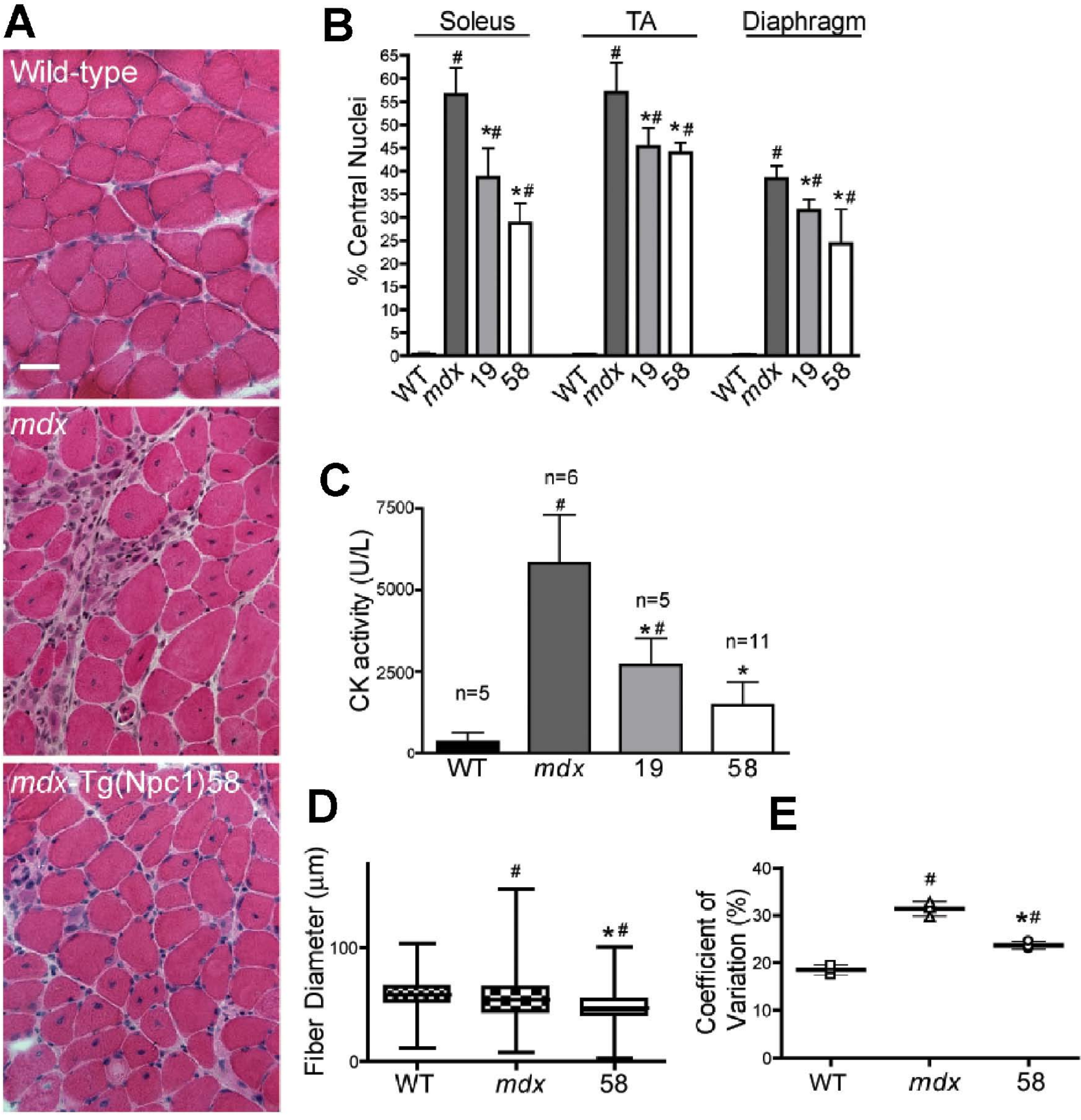
A
Wild-type
mdx
mdx-Tg(Npc1)58
B
Soleus
TA
Diaphragm
% Central Nuclei
WT
mdx
19
58
C
CK activity (U/L)
n=6
n=5
n=5
n=11
D
Fiber Diameter (µm)
E
Coefficient of Variation (%)